

The Role of the Spherical Tokamak in the U.S. Fusion Energy Sciences Program

Organized by J. Menard with contributions from the NSTX-U research team and US ST community members

This whitepaper is meant to serve as a resource to the FESAC subcommittee to provide information on the progress, goals, and plans for how the U.S. ST community will support fusion energy science in the next decade. This whitepaper is organized into 5 sections. The first two sections provide 1) perspective and 2) motivation for ST research. Sections 3-5 address the FESAC charge questions and describe: 3) support of burning plasma science for ITER, 4) utilization of the ST to address critical challenges for long-pulse/steady-state operation including plasma-wall interactions, and 5) utilization of the ST to advance fusion materials science and harness fusion power.

1. Perspective

The U.S. fusion program presently possesses a world-leading spherical tokamak (ST) program embodied in three facilities including the National Spherical Torus eXperiment (NSTX) at PPPL and the smaller Pegasus Toroidal Experiment (University of Wisconsin) and Lithium Tokamak eXperiment (LTX - also at PPPL). The NSTX facility is presently undergoing a major upgrade scheduled to be completed in 2014. The upgraded NSTX (NSTX Upgrade¹) will double the toroidal field, plasma current, and heating power, increase the pulse duration by a factor of five, and will significantly extend non-inductive current drive studies to full non-inductive ramp-up and sustainment, access up to an order of magnitude lower collisionality, and test novel plasma-material-interaction (PMI) solutions for a Fusion Nuclear Science Facility (FNSF) and Demo including high-flux-expansion divertors and liquid metals. The Pegasus Toroidal Experiment is leading research in point helicity injection plasma current formation for solenoid-free plasma start-up for next-step STs, and LTX is leading innovative research on liquid metal solutions for plasma facing components and plasma confinement optimization. For next-step fusion applications in the U.S., the high beta, compact geometry and high power density, accessibility, modularity, and simplified magnets of the ST are potential advantages for plasma material interaction and material studies and for a compact FNSF. Longer term, the resistive dissipation in the toroidal field of a normally conducting ST power plant² or pilot plant³ is generally a disadvantage for electricity production. However, the ST ($A < 2$) can strongly inform the physics performance of reduced aspect ratio ($A=2-2.6$) super-conducting Demo concepts studied in Japan that are projected to minimize device mass, cost, and radioactive waste^{4,5,6,7}. The U.S. should sustain its leadership-class ST program in the coming decade to extend the unique plasma parameter range provided by the ST, utilize this capability to support ITER and the development of predictive capability for burning plasmas, and to provide potentially attractive options for U.S. next-step facilities such as a Fusion Nuclear Science Facility (FNSF).

2. Motivation for ST Research

The Spherical Torus/Tokamak (ST) is a low-aspect-ratio tokamak magnetic configuration characterized by strong intrinsic plasma shaping and enhanced stabilizing magnetic field line curvature. These unique ST characteristics enable the achievement of a high plasma pressure relative to the applied magnetic field and provide access to an expanded range of plasma parameters and operating regimes relative to the standard aspect ratio tokamak. NSTX has demonstrated that ST's can access a very wide range of dimensionless plasma parameter space with toroidal beta up to 40%, normalized beta up to 7, plasma elongation up to 3, normalized fast-ion speed $V_{fast}/V_{Alfvén}$ up to 5, Alfvén Mach number $M_A = V_{rotation}/V_{Alfvén}$ up to 0.5, and trapped-particle fraction up to 90% at the plasma edge. All of these parameters are well beyond that accessible in conventional tokamaks, and these parameters approach

those achievable in other high-beta alternative concepts. Further, it is also possible and common to overlap with conventional aspect ratio tokamak physics parameters. These characteristics therefore allow ST research to complement and extend standard aspect-ratio tokamak science while providing low-collisionality, long pulse-duration, and well-diagnosed plasmas to address fundamental plasma science issues – including burning plasma physics in ITER.

3. Support of Burning Plasma Science for ITER

3.1. Fast-ion confinement in the presence of Alfvénic instabilities driven by alphas, NBI fast ions and RF waves

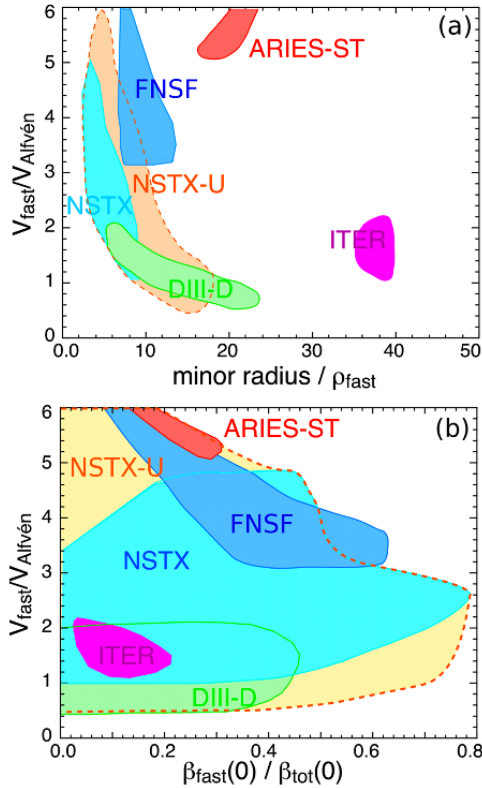


Figure 1 - Relevant parameters for Energetic Particles research for existing US tokamaks in comparison with expected values for ST-based reactors (FNSF, ARIES-ST) and for ITER. (a) Ratio of fast ion to Alfvén velocity vs. inverse of the normalized fast ion Larmor radius. (b) Ratio of fast ion to Alfvén velocity vs. ratio of fast ion to total pressure

The fundamental scientific goal of ITER is to generate plasmas dominated by alpha particle heating and to understand the dynamics of the thermal and energetic plasma particles under such conditions. The dynamics is potentially non-linear, since a relatively large population of energetic ions originates from fusion reactions (alpha particles), Neutral Beam (NB) injection and injected RF waves⁸. The resulting fast ion pressure can destabilize Alfvén Eigenmodes (AEs) that, in turn, affect the fast ion distribution through enhanced transport in space and energy^{9,10}. This may cause unpredictable variations in the NB-driven current profile¹¹, loss of macroscopic stability¹² and degraded performance. Energetic Particles (EP) research is paramount to understand the coupled dynamics of fast ions and AE instabilities and eliminate or minimize their potential harm to a reliable exploitation of fusion energy. The challenge for present tokamaks is to provide the required physics basis to enable the development, verification and validation of predictive theoretical and numerical tools.

In the past years, NSTX experiments have considerably broadened and enriched the fusion science with respect to EP physics. Besides advancing the characterization of known instabilities such as the Toroidal Alfvén Eigenmode^{13,14,15} (TAE), new instabilities and new aspects of AE physics and associated fast ion transport have been discovered^{16,17,18,19,20,21}. Phenomena that are potentially

harmful to ITER and burning plasma devices have been investigated in detail. For instance, TAE modes can develop into a non-linear regime²² characterized by frequent, rapid bursts (*avalanches*) that result in a fractional loss of fast ions^{23,24,25} in excess of 10% and a prompt redistribution of NB-driven current⁴. Such observations may project unfavorably to ITER scenarios with super-Alfvénic NB ions that provide further drive in addition to alphas for TAE instabilities³, since no control tools are available (or envisioned) to suppress or mitigate avalanching modes occurring on time-scales of 1-10 ms. NSTX-U will encompass an even broader parameter space than NSTX²⁶, see Fig. 1. The capability of spanning a much broader range

of parameters for EP physics than conventional tokamaks represents an important advancement for extrapolations from today's experiments to burning plasma regimes.

EP research in the initial 5 years of NSTX-U operations will focus on two high-level goals that will directly contribute to the development of predictive capability for FNSF, ITER and future devices. Firstly, tools and techniques to affect AE and fast ion dynamics through selective excitation/suppression of fast ion-driven instabilities will be assessed. This requires a detailed study of AE drive and damping mechanisms and of the fast ion response to different instabilities. Upgraded diagnostics (e.g. reflectometer arrays²⁷, beam-emission spectroscopy²⁸, fast-ion D-alpha spectrometers^{29,30}, neutral particle analyzers^{31,32} and fusion product profile arrays³³) are being developed to provide a detailed description of the mode dynamics and of the properties of confined fast ions. The possibility of exploiting instabilities to modify the NB-driven current profile or enhance the energy transfer from NB ions to thermal ions in a controlled way³⁴ will also be explored. The possibility of regulating the electron thermal transport through high-frequency modes¹⁰ will be also pursued. NB and RF injection are the primary actuators. For a more refined mode control, a dedicated antenna system will be developed to excite/stabilize specific modes, based on the broad radial structure and finite edge amplitude of AE modes in typical ST scenarios. Secondly, experiments in the upgraded machine will aim at extensive validation of both linear and non-linear numerical codes and models, taking advantage of the upgraded NSTX-U diagnostic tools for stringent theory/experiment comparisons. This will enable projections of fast ion transport and AE dynamics from present experiments to scenarios relevant for FNSF, ITER and a ST-based Pilot device and provide guidance for further improvements in the design of future reactors.

3.2. Impact of micro-tearing and other micro-instabilities on electron transport

Understanding electron thermal transport is a critical element for magnetic fusion research, since electron energy loss can be the dominant loss mechanism in magnetically confined plasmas. While electrostatic turbulence mechanisms are generally expected to be dominant in ITER, magnetic turbulence driven by microtearing modes is also being investigated as a possible contributor. Recent theoretical work has found that microtearing modes (fundamentally a magnetic turbulence mechanism) can lead to significant electron thermal transport in conventional aspect ratio tokamaks³⁵. Calculations based specifically on model ITER plasmas have also predicted microtearing to be unstable in the pedestal region³⁶. Microtearing modes are expected to dominate in high beta spherical tokamaks such as NSTX and MAST, and are also shown to be important in some RFP plasmas. Consequently, understanding the effects of magnetic turbulence from microtearing modes is important both directly for ITER and indirectly through the broader magnetic confinement research program.

Past NSTX research has contributed significantly to improving the understanding of microtearing transport. Linear analysis has clarified key parametric dependencies to determine when and where it is important³⁷, and model predictions have demonstrated the resulting transport should be significant in NSTX³⁸. Recent nonlinear simulations confirm these model predictions³⁹ and also predict transport that scales consistently with the observed energy confinement⁴⁰, confirming microtearing turbulence as an important transport component. NSTX-U provides a unique opportunity to advance understanding of microtearing turbulence for both STs and the broader MFE community. A newly implemented diagnostic⁴¹ will allow for the measurement of internal magnetic fluctuations fundamental to microtearing turbulence. Coupled with other upgraded diagnostic capabilities it should be possible to establish a direct link between magnetic turbulence and transport. In addition, the facility upgrades of NSTX-U provide a significantly broader achievable range of parameter space allowing the above investigations to overlap both high beta ST-relevant regimes and lower beta regimes relevant to ITER and FNSF. Access to

reduced collisionality is an especially important attribute of NSTX-U, since the microtearing thermal diffusivity is proportional to the electron collisionality. Reduced and controllable microtearing transport should also help elucidate the relative importance of electron temperature gradient (ETG)^{42,43,44,45} and global Alfvén eigenmode (GAE)^{46,47} induced turbulence previously shown to be important in NSTX plasmas.

3.3. Ion-Cyclotron Range-of-Frequency coupling, heating, and edge losses

Radiofrequency heating in the ion-cyclotron range of frequencies (ICRF) will be a primary heating scheme on ITER; 20 MW are currently being planned. Important ICRF issues include achieving sufficiently high coupling from the antenna to the plasma while simultaneously avoiding deleterious effects such as impurity release or overheating of plasma-facing components. However, a different sort of loss mechanism is apparent in NSTX: a major loss of high-harmonic fast wave (HHFW) power can occur along open field lines passing in front of the antenna over the width of the scrape-off layer (SOL), as shown in Figure 2. In such cases, the heating efficiency has been shown to be related to the location of onset density for perpendicular fast wave propagation, and it is hypothesized that surface waves are being excited just beyond this onset density^{48,49}. This hypothesis is supported by the observation that the flow of HHFW power is aligned along magnetic field lines that pass in front of the antenna throughout the radial width of the SOL⁵⁰. If true, this suggests that this loss mechanism, distinct from the well-studied losses occurring directly at the antenna components, is common to different degrees in ICRF heating schemes. On NSTX-U, the increased magnetic field strength will enable greater exploration of the effects of the location of the onset density, while more detailed diagnostic measurements will confirm whether or not strong RF fields are present in the SOL. Whatever the underlying mechanism, these results should serve to determine the validity of advanced RF code simulations of the RF edge power deposition in the SOL⁵¹ with respect to power flow along the open field lines passing in front of the antenna. These codes can then be combined with edge RF field measurements to predict and minimize such edge losses in the ICRF heating regime. Fully understanding the underlying mechanisms behind this loss is critical for optimizing HHFW performance and fast wave performance generally, especially for high-power long-pulse ICRF heating on ITER, while guarding against excessive erosion in the divertor region.

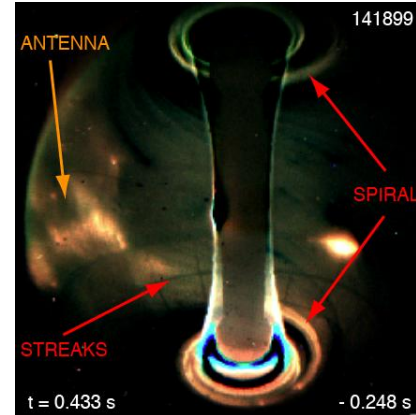


Figure 2 - During RF heating on NSTX, bright streaks can emerge from the antennas and terminate in bright and hot spirals in the upper and lower divertor regions, indicating that a significant fraction of the RF power couples directly to the SOL and is subsequently lost to the divertor regions.

3.4. Accessing the high-confinement mode (H-mode)

As the target operating mode in ITER will be the H-mode, it is imperative to understand the conditions for minimizing the power requirements for transition into the H-mode. This knowledge will aid in the development of a sensible research plan as well as guide the requirements for phasing in the necessary auxiliary heating power. The work on NSTX and NSTX-U impacts not only ITER requirements, but also those for a successful FNSF, ST-based or not, as well. Previous studies of the L-H transition on NSTX^{52,53} focused first on the species dependence of the threshold power, addressing the ITER proposal to operate with helium plasmas prior to D-T operation. As such, NSTX used High Harmonic Fast Wave (HHFW) RF heating (no particle fueling) to assess the difference in P_{LH} between relatively pure deuterium and

helium plasmas. This work was part of a joint ITPA effort being carried out on multiple devices. NSTX found that that $P_{\text{LH}}(\text{He})$ was only ~20% greater than that for deuterium, consistent with results from other devices. This result allowed the ITER design team to start developing scenarios for helium H-mode operation with its planned auxiliary heating systems. Additional experiments were carried out in deuterium plasmas with applied 3D magnetic perturbations, which ITER may use for ELM suppression. The NSTX results indicated much higher threshold powers with modest 3D $n=3$ perturbations applied than without. This has major ramifications on how ITER can operate its ELM-suppression coils, should they be installed. It will be necessary to apply the 3D perturbations only after the discharge has transitioned into the H-mode to minimize the required threshold power.

Operation in NSTX-U will extend these studies into lower collisionality and toroidicity regimes that will be closer to those of both ITER and FNSF. HHFW power can be used again to assess the species dependence of the threshold power to confirm that helium operation in H-mode is feasible. The added flexibility planned with a new set of non-axisymmetric magnetic field perturbation coils, able to apply fields with toroidal structures up to $n=6$, will test the dependence of the threshold power on these higher n applied fields. Studies will also be carried out to assess whether there is any hysteresis effect of applying the perturbed fields just after the discharge has transitioned into the H-mode. Will the discharge remain in H-mode, or will it fall back into L-mode? Such studies can be carried out by implementing a control algorithm that will sense the L-H transition and then apply the perturbed fields.

3.5. Mitigation of Edge Localized Modes (ELMs) during H-mode Operation

The performance of tokamak fusion power plants (e.g., ITER) is known to depend sensitively on the H-mode pedestal parameters. More specifically, using transport models⁵⁴, a pedestal temperature of 4 keV has been predicted for ITER. High pedestal temperatures, however, are typically accompanied by instabilities (type I ELMs), which substantially exhaust a large fraction of the plasma stored energy onto the plasma facing components (PFCs). For large heat loads exceeding the PFC power handling capabilities, the PFCs would melt. Hence, ELM mitigation is an important and active research area for ITER and FNSF. Mitigation approaches include the application of 3D fields, which were found to suppress ELMs on DIII-D⁵⁵ and ASDEX⁵⁶, and were found to controllably trigger ELMs on NSTX⁵⁷. Triggering ELMs to avoid exhaust of large energy onto the PFCs, was also proven using injection of deuterium pellets, and recently by injection of Lithium granular pellets on EAST utilizing an injection system developed for NSTX.

3.5.1. ELM control using externally applied non-axisymmetric (3D) magnetic fields

Another method for controlling ELM size is through the application of 3D magnetic fields. While this approach has demonstrated the mitigation or suppression of ELMs on several experiments, the underlying physics remains elusive and so substantial uncertainty exists in extrapolating this technique to ITER. In NSTX experiments, it was found that applied 3D fields did not mitigate or suppress ELMs, but instead destabilized them, causing ELMs to be triggered in otherwise ELM-free H-modes⁵⁷. While this result highlights that further progress is needed in understanding the impact of 3D fields, the ELM-triggering effect has also opened the possibility of using 3D fields to pace ELMs and reduce their size⁵⁸. Studies of the physics of how 3D fields affect ELM behavior will be enhanced on the NSTX-Upgrade, where improved edge diagnostics will allow more precise measurements of, e.g., pedestal structure changes with 3D fields. Further, the reduced collisionality plasmas anticipated in the Upgrade may allow access to regimes where the pedestal transport response to 3D fields is more pronounced⁵⁹, and will improve cross-machine comparisons with low-collisionality ELM suppression experiments at DIII-D. Finally, an

upgraded 3D coil set would greatly enhance the flexibility and control of the perturbation characteristics. This will give an opportunity to experimentally separate resonant effects such as island formation from non-resonant effects (e.g., neoclassical toroidal viscosity⁶⁰). With the ability to better discriminate between physics effects, the Upgrade would substantially contribute to the physics basis for projecting the impact of 3D fields on edge stability in burning plasma devices.

3.5.2. ELM control using lithium-based plasma facing components

Another possible means of ELM control is through the use of lithium. In NSTX experiments, it was shown that applying progressively thicker lithium coatings to the PFCs reduced the ELM frequency⁶¹, and with enough lithium ELMs were eliminated altogether⁶². With thick lithium coatings, the pressure gradient and bootstrap current were reduced near the separatrix, so that peeling-ballooning modes were stabilized. At the same time, the pedestal broadened substantially, so that higher pedestal-top pressures were achieved⁶³. An added benefit of this approach to ELM control is the continuous increase in energy confinement that has been observed as the amount of lithium applied to the PFCs is increased⁶⁴. The effects of lithium coatings will continue to be studied in the NSTX-Upgrade, including testing the saturation of energy confinement improvement as more lithium is put into the machine (this has not been observed in NSTX experiments to date). These studies will help quantify the respective roles of lower collisionality and plasma-wall interactions in controlling confinement. Further, the enhanced pedestal and divertor diagnostics will allow the detailed mechanisms of recycling and transport changes thought to be responsible for the ELM stabilization to be probed. This, coupled with continued theoretical efforts to understand the plasma response to lithium, will allow the effects of lithium to be projected for future devices such as ITER and/or FNSF, and provide the basis for evaluating its use for ELM control.

3.5.3. ELM control using ELM pacing using a lithium granule injector

While ELM suppression is generally favored, ELM mitigation remains a viable option on NSTX-U and could be the preferred approach for ITER and FNSF. Deuterium pellet injection has been routinely used to trigger ELMs⁶⁵, and such injection tends to contribute to the plasma fueling and increased collisionality. A new approach using granule injection of lithium (developed at PPPL) has recently been successfully tested on EAST. This approach consists of redirecting (radially into the plasma) a stream of falling lithium granules using a rotating impeller. The preliminary results show the triggering of ELMs using pellets of 0.7 mm diameter, which are propelled at a speed of 52 m/s. In addition, a conversion efficiency (ratio of propulsion of granules to ELMs triggered) of approximately 100% was demonstrated. The triggered ELMs are observed to be smaller than the naturally occurring ELMs. With this proof-of-principle demonstrated on EAST, ELM mitigation using lithium granules will be a key component of the NSTX-U research program. This capability will be utilized in concert with the ongoing lithium PFC program and could prove to be a very powerful means of controlling ELMs, i.e. using lithium to both suppress and trigger ELMs on command. The efficacy of using this technique to mitigate ELMs in low collisionality regimes, closer to those of next step devices such as FNSF and ITER, will be investigated.

3.6. Steady-state divertor heat flux mitigation

Normal and off-normal heat and particle flux mitigation and control strategies beyond those used in present devices, and/or envisioned for near-future devices, such as ITER, must be developed. Candidate techniques for steady-state mitigation of divertor heat and particle loads in future fusion plasma devices must be capable of reducing particle fluxes to the levels of acceptable divertor plate material erosion rates and heat fluxes down to $q < 10 \text{ MW/m}^2$, a limit imposed by the present day divertor material and cooling

constraints. The techniques must also be compatible with high-performance high-confinement (H-mode) core plasma, favorable edge pressure for an attractive ELM regime, and particle control methods. At present, candidate mitigation strategies for ITER and next step fusion devices (e.g., DEMO) include both the passive techniques, such as the divertor geometry and magnetic balance, and active techniques, such as the radiative divertors, field ergodization and strike point sweeping.

3.6.1. Radiative divertors using deuterium and lithium

Radiative divertors use deuterium and/or seeded impurities to reduce divertor particle and heat fluxes through volumetric momentum and energy dissipative processes - the ion-neutral elastic and inelastic collisions, recombination and radiative cooling. The radiative divertor has been demonstrated to reduce peak divertor heat flux by large amounts (factors of 2-5) with the divertor radiated power fractions approaching 50 % of input power while maintaining good H-mode confinement.

Owing to its inherently compact ST divertor, NSTX demonstrated ITER-level steady-state divertor peak heat fluxes ($q < 10\text{-}15 \text{ MW/m}^2$), making it a good testbed for studying divertor heat flux mitigation scenarios utilizing divertor geometry effects and radiative solutions. Experiments conducted in high-performance 1.0 and 1.2 MA 6 MW NBI-heated H-mode discharges in NSTX with a high (16-25) magnetic flux expansion radiative divertor demonstrated that significant divertor peak heat flux reduction, from 6–12 to 0.5–2 MW/m^2 , through partial strike point detachment could be obtained in a compact divertor of a high power density ST even with only deuterium gas and carbon radiation^{66,67,68}.

For steady-state high-performance operation, however, steady-state radiative divertor conditions must be sustained. This can be accomplished by feedback through controlling the rate of injection of the deuterium or impurity gas, using some divertor parameter as a control quantity. Research planned for NSTX-U will include radiative divertor experiments with impurity seeding, as well as the development of radiative divertor scenarios with feedback control. A number of divertor measurements that would be available in NSTX-U can be used as a control signal⁶⁹. Ultimately, the developed radiative divertor scenario must be combined with the particle control solution, e.g. a cryogenic divertor panel in ITER, and/or with lithium plasma-facing component coatings, and this will be tested in NSTX-U.

3.6.2. Impact of 3D magnetic field ELM control on radiative divertors

An important consideration for the usage of 3D fields for ELM control in ITER is the impact of these fields on peak heat and particle fluxes in the divertor. In particular, ELM mitigation using the 3D fields and heat flux reduction using a radiative divertor (i.e. detachment) discussed above must be compatible with each other. Importantly, results from NSTX have shown that divertor detachment can be spoiled, *i.e.* plasma reattaches, by the applied 3D fields ($n=3$). However, this can be avoided when the detachment is enhanced by puffing sufficient gas into the divertor region. TRANSP analysis of NSTX results showed that the decrease of pedestal electron heat diffusivity (χ_e) by the applied 3D fields leads to an increase of electron temperature (T_e) that leads to the reattachment of divertor plasma (see Figure 3). It is not yet understood why under these conditions the 3D fields lead to reduced χ_e and higher T_e in the edge region.

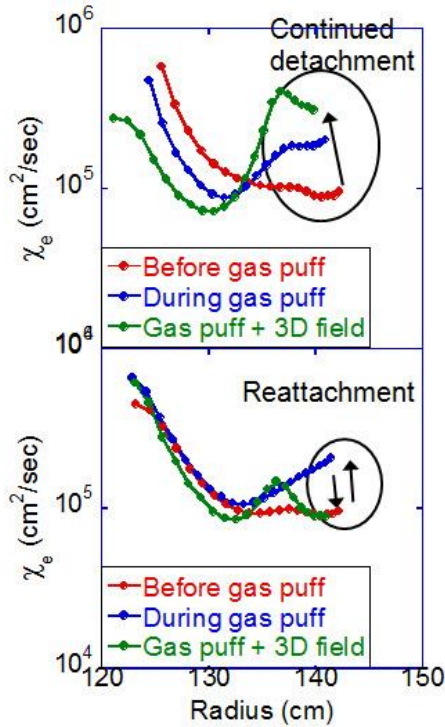


Figure 3 - Evolution of pedestal χ_e profile for high (upper) and low (lower) divertor gas puff with 3D fields applied later during the detached phase.

The higher NBI power ($P_{\text{NBI}} \leq 10\text{MW}$) and plasma current ($I_p \leq 2\text{MA}$) of NSTX-U will dramatically raise the peak heat flux; therefore, detachment by the snowflake divertor and the divertor gas injection will be pursued to deal with this challenge. 3D fields from the proposed non-axisymmetric control coil (NCC) will present an opportunity to investigate the impact on the divertor detachment with significantly wider field spectra. An important advantage of NSTX-U is the broader range of pedestal collisionality (ν_e^*) and q_{95} . Whether the lower pedestal collisionality can be sustained with the increased divertor collisionality necessary for the achievement of detachment and how they are influenced by 3D fields will be examined in detail. This will greatly improve our understanding about the role of collisionality in the transport processes responsible for the interaction between 3D fields and detachment. Lower q_{95} leads to less strike point splitting and vice versa, but its effect on detachment is yet unclear. The answer to how q_{95} variation, along with the impact on ELM mitigation, would enhance or spoil detachment will contribute to unveiling the underlying physics as well as to the development of ST operation scenarios. The open geometry of the NSTX-U divertor will also allow for easier investigation of toroidally asymmetric heat deposition by ELMs and 3D fields^{70,71}, therefore its relationship with detachment, using the 2D high speed IR camera⁷² and 3D heat conduction solver⁷³. Lastly, the longer pulse length (up to 5 sec) and the improved

steady state capability will enable us to look into the spatial and temporal propagation of the associated physics processes.

3.7. Control and correction of 3D magnetic field errors (“error fields”)

Non-axisymmetric error fields almost always exist in tokamaks, due to imperfections in the primary magnets and surrounding conducting structures. This error field should be properly controlled, since otherwise an error field as small as $\delta B/B=10^{-4}$ can induce the formation of locked magnetic islands which at best degrade confinement, and at worst can lead to a major disruption. This issue is especially important for ITER, since ITER plasmas will likely have low toroidal rotation and may be very sensitive to error fields and mode locking.

3.7.1. Inclusion of plasma response to 3D fields for ITER error field correction

The key to the successful error field control is to understand the interaction between the tokamak plasma and non-axisymmetric perturbations, namely, the plasma response to error fields. NSTX research on error field physics was the first to highlight the importance of plasma response by demonstrating that error fields from the inboard can be compensated by the 3D correction coil fields from the outboard, but only with a significantly different direction of correction compared with the conventional method without plasma response^{74,75}. The Ideal Perturbed Equilibrium Code (IPEC)⁷⁶, which was developed to precisely calculate the plasma response, has been successfully applied to NSTX and many conventional aspect ratio

tokamaks. IPEC applications provided the error field threshold scaling across tokamaks, as shown in Figure 4, and IPEC-derived results are presently being used for ITER error field correction⁷⁷. However, an important issue still remains, as the non-resonant error field can indirectly affect the plasma performance by causing unnecessary non-ambipolar plasma transport⁷⁸. The non-resonant error field physics is more complicated and is highly dependent on plasma parameters such as collisionality. NSTX-U will provide significantly improved capabilities to explore and study such non-resonant field effects, with collisionality values closer to those of next-step STs and to ITER. Furthermore, if the proposed Non-axisymmetric Control Coil (NCC) upgrade becomes available, the wider ($n=1-6$ vs. present $n=1-3$) and more flexible spectrum (off-midplane vs. present mid-plane) of the 3D fields from the NCC will enable improved ability to distinguish between non-resonant vs. resonant error-field physics in support of ITER and next-steps.

3.7.2. Intrinsic rotation physics

Intrinsic toroidal rotation and torque are important subjects in tokamaks as they are expected to play a dominant role in establishing toroidal rotation in ITER. The toroidal rotation, and its shear across the plasma region, can strongly influence various instabilities from macroscopic scale to microscopic scale such as turbulence, and therefore better understanding of intrinsic toroidal rotation can lead to improved stability predictions in ITER. The study of intrinsic rotation is inevitably coupled to the study of other toroidal momentum transport in general, as they can interact and exchange the momentum locally and globally as a sink or a source. NSTX research first experimentally demonstrated the momentum inward pinch effects, as theory predicted, as opposed to the conventional momentum outward diffusion^{79,80}. These momentum exchange effects cannot provide the toroidal torque, but can alter the rotation profile and stability with the momentum sources such as the intrinsic torque. On the other hand, the study of intrinsic torque should properly decouple these momentum exchange effects. NSTX research contributed to the intrinsic rotation physics understanding, with careful considerations on other momentum transport effects, and by showing the correlation with ion temperature gradient as the corresponding theory predicted⁸¹. Furthermore, unique ST features such as high magnetic shear have been found to be important, indicating that NSTX-U can provide unique contributions to intrinsic rotation physics in toroidal confinement devices. Presently available and planned diagnostics in NSTX-U, such as passive charge exchange recombination diagnostics and a X-ray crystal spectrometer, will also enable NSTX-U to study the intrinsic rotation without neutral beam injection and thus without any momentum injection.

3.8. Disruption detection, avoidance, and mitigation

ITER must operate with a very low disruption rate, and when disruptions are imminent, they must be detected with a very high degree of reliability. NSTX was a pioneer in error field control techniques relevant to disruption avoidance in all ITER scenarios, and RWM control techniques critical for the 100% non-inductive advanced scenarios in ITER and for FNSF. Recently, NSTX research has begun to assess disruption detection techniques for ITER, FNSF, and NSTX-Upgrade.

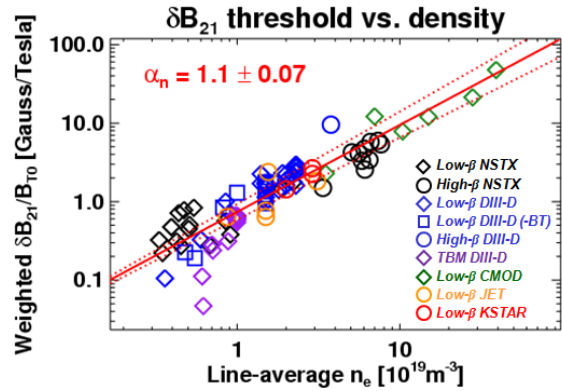


Figure 4 - Multi-machine scaling across tokamaks for error field threshold for locking instability.

While NSTX has verified that a large fraction of disruptions can be predicted via these signals, we have attempted to use additional physics signals & analysis to look for precursors. As an example, there are often large anomalies in the neutrons emission during the phase leading to a disruption. We take the ratio of the measured neutrons to the prediction from a 0D NBI slowing-down model, and find that when that ratio becomes sufficiently small, a disruption is imminent. Figure 5 shows that when that ratio drops beneath 0.4, a disruption typically occurs within 100ms, and almost always within 200ms. Other precursors considered in NSTX analysis include loop voltage anomalies, vertical motion signatures, and rotation signatures.

NSTX-Upgrade will expand on this research, in order to both improve operational efficiency and to lay the groundwork for FNSF. An assessment of required real-time diagnostics for on-line disruption detection will occur as part of an FY-13 research milestone. These diagnostics will be brought on line through the subsequent research period. However, initial real-time disruption detection work utilizing the presently available RWM and vertical motion detectors will be initiated immediately upon resumption of operations. These will be coupled with strategies for termination of the discharge, via a controlled shut-down or massive gas injection.

At present, Massive Gas Injection (MGI) is the most promising method for safely terminating disruptions in ITER. Because of the large minor radius of ITER, the long transit times for the slow moving neutral gas, and the large scrape-off-layer flows, it is not known if a simple MGI pulse would be adequate for safely terminating a discharge. While MGI experiments are being conducted at a number of tokamak facilities, the impact of varying the poloidal injection location has not been adequately studied, and injection into the private flux region has not been studied.

Additional insight into ways for reducing the total amount of injected gas and appropriate injection locations would further help optimize the MGI system for ITER. NSTX-U will study this aspect of MGI by varying the poloidal gas injection location on the efficiency of injected gas assimilation by the tokamak discharge, and the resulting dynamics of the thermal quench phase. In particular, NSTX-U will offer new data by injecting gas into the private flux region and into the lower X-point region to determine if this is a more desirable location for massive gas injection. Comparisons with an un-mitigated disruption will be used to assess reduction of divertor heat loads and halo currents.

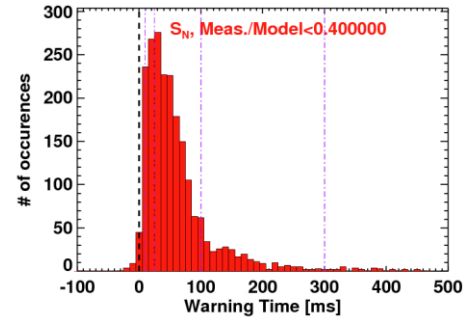


Figure 5 - Histogram of disruption warning times, where the ratio of measured to modeled neutrons dropping beneath 0.4 is considered the precursor.

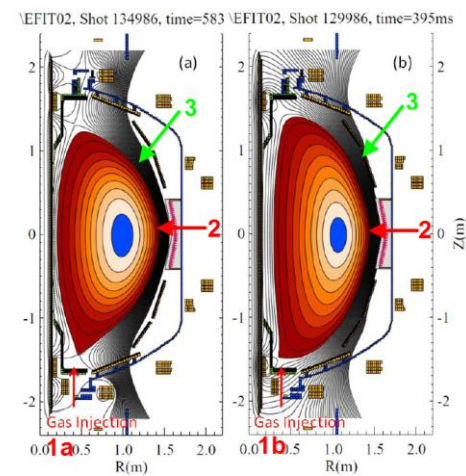


Figure 6 - Planned Massive Gas Injection locations on NSTX-U. (1a) Private flux region, (2) mid-plane injection, (1b) high field lower SOL region and (3) outer SOL above the mid-plane.

Injection from this new location has two advantages. First, the gas will be injected directly into the private flux region, and so it does not need to penetrate the scrape-off-layer region. Second, because the injection location is near the high-field side region, the injected gas should be more rapidly transported to the interior as known from high-field side pellet injection research and from high-field side gas injection on NSTX-U. By comparing gas injection from this new location to results obtained from injecting a similar amount of gas from the conventional outer mid-plane region and from other poloidal locations, NSTX-U results on massive gas injection will extend the multi-machine disruption database for improving computational simulations and add new knowledge to disruption mitigation physics using massive gas injection. Figure 6 shows the proposed injection locations for NSTX-U. Other methods for disruption mitigation based on CT injection and particle injection are in early stages of development by NSTX collaborators and could be considered for tests on NSTX-U (*see whitepapers by R. Raman*).

3.9. Support of ITER Advanced Scenarios

3.9.1. Full non-inductive current drive operation

Non-inductive scenarios in ITER will typically operate with ~20% of their current driven by off axis-neutral beams. NSTX has extensively studied neutral beam current drive^{82,83}. While it was found that the NBCD is typically classical in configurations without large MHD, it was found that core kink/tearing modes^{82,83} or TAEs⁸⁴ could lead to large redistribution of the NBCD. For instance, the upper frame of Figure 7 shows a TAE avalanche example where the current profile reconstructed from MSE constrained Grad-Shafranov codes (black) is much less peaked than that computed as the sum of classical current drive sources (green). However, when impulsive fast ion losses, whose magnitude was set to match the dynamics of the neutron losses, are added to the simulation, the two calculations of the current profile agree quite well. NSTX-Upgrade will be uniquely positioned to add to this understanding. The additional neutral beam lines mean that the NBCD can be a larger part of the total current balance, increasing the sensitivity of the equilibria to small variations in the anomalous diffusion. This will in turn enable better benchmarking of the classical beam current drive calculations, and a better assessment of the impact of *AE modes.

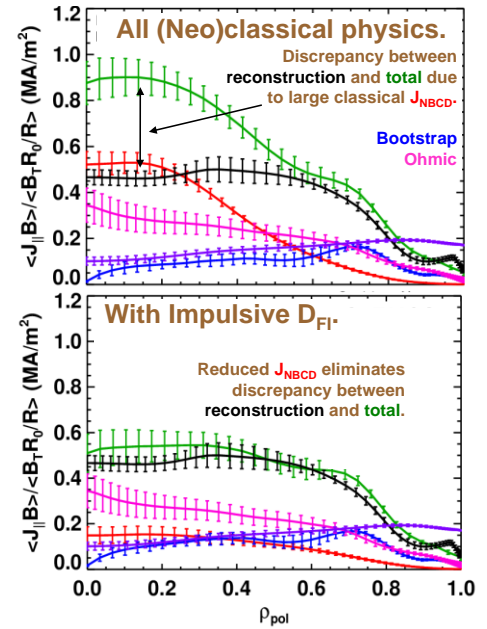


Figure 7 - Current profile calculations using all neoclassical physics (top), and with bursts of anomalous fast ion density mimicking the effect of TAE avalanches (bottom).

3.9.2. Resistive wall mode stability and control

Advance operating scenarios in ITER relying on full non-inductive current drive will necessarily operate above the no-wall kink stability limit. Passive conductors, such as the blanket shield modules and vacuum vessel, can provide wall stabilization to slow kink-mode growth from micro-seconds to the resistive-wall field penetration time-scale of milliseconds resulting in a resistive wall mode (RWM). Passive stabilization of the RWM via either externally driven or intrinsic rotation combined with kinetic dissipation may provide stabilization of the RWM, but such damping is highly profile-specific, and active RWM control may be required for reliable operation of ITER above the no-wall limit.

Resistive wall mode (RWM) research in NSTX-U aims to improve the reliability of long-pulse, high performance operation, and to understand the key physics needed to extrapolate such operation to the reduced plasma collisionality and internal inductance needed for future devices including ITER. The characteristics of the unstable RWM at low aspect ratio are well documented in NSTX. Early work determined that the RWM eigenfunction is ballooning in nature with the largest perturbation on the outboard side and that the mode effectively couples to the passive stabilizing plates. This investigation included a physics design of an active stabilization control system for the device⁸⁵. Error field reduction resulted in a large stabilized operating space with $\beta_N / \beta_N^{\text{no-wall}}$ up to 1.5 at the highest β_N values reached in the device.⁸⁶ Maintaining toroidal plasma rotation across the entire profile led to passive RWM stability.⁸⁷ Unstable RWMs with toroidal mode number up to three were observed in NSTX for the first time in a tokamak experiment.

Significant progress has been made in identifying passive stabilization physics consistent with unique observations on NSTX. For instance, RWM instability at intermediate levels of plasma rotation is observed on NSTX, and is associated with the plasma rotation profile moving between bounce frequency and ion precession drift resonances^{88,89}. The role of collisionality is also initially studied in these references. The role of energetic particles is also being investigated in NSTX.⁹⁰ Research in NSTX-U will continue to establish this physics, with the goal of forming a physics model that unifies results across machines for more confident extrapolation to future devices including ITER.

Another significant milestone was the first active stabilization of the resistive wall mode (RWM) at low aspect ratio, and at reduced plasma rotation applicable to ITER.⁹¹ Most recently, an advanced state-space RWM controller was implemented for NSTX and initial experiments using this controller were conducted. Research in NSTX-U will further use and develop this controller to improve RWM control systems that aim to allow control coils to be placed further away from the plasma, yet remain effective^{92,93}.

For additional info on NSTX/NSTX-U advanced stability control and support of advanced operating scenarios, please refer to the whitepaper submitted by S. Sabbagh and J. Berkery of Columbia University.

4. Utilization of the ST to address critical challenges for long-pulse/steady-state operation including plasma-wall interactions

4.1. Demonstrate and quantify sustained 100% non-inductive fraction plasma scenarios

It is generally accepted that a fusion nuclear science facility must operate steady state, with high neutron wall loading, for pulses of many days or weeks in duration. NSTX research demonstrated sustained high-

β_N operation with non-inductive fractions $>65\%$, a vital step along the path to an ST-FNSF. An example of this discharge type is shown in Figure 8, where this 750 kA discharge is maintained at high β_N for many current redistribution times^{94,84}; the discharge is limited by the duration of the toroidal field flat-top, not by any MHD instabilities. NSTX-U will take another large step toward these goals.

There are a number of key questions for the FNSF operating space whose answers will be explored in NSTX-U. For the ST version of an FNSF, we need better understanding of the confinement scaling to higher field and current under relevant high-performance conditions. NSTX-U will be very sensitive to these operation points: the non-inductive current level at full power and $B_T=1.0$ T will be ~ 1 MA under ITER-98y,2 scaling, but 1.3 MA under some recently quoted ST scalings⁹⁵. Hence, the proper scaling to use should become more clear. It is also interesting to understand the optimal q -profile for high-performance 100% non-inductive operation. For instance, higher q_{\min} may be natural for near fully bootstrap driven systems, and have some optimal stability properties. However, the transport may be best (smallest) when q_{\min} is closer to unity. By varying which neutral beam sources are used, NSTX can vary the balance of current drive sources, thus scanning q_{\min} at fixed I_p .

For example, Figure 9 shows q_{\min} varying between 1.1 and ~ 2.5 with very high non-inductive fraction, with all parameters fixed except for the NB source selection. Experiments using this flexibility will be used to determine the optimal q_{\min} . Furthermore, this capability will be used to develop feedback controllers on q_{\min} , enabling the optimal q -profile to be maintained in NSTX-U and, in the future, an FNSF.

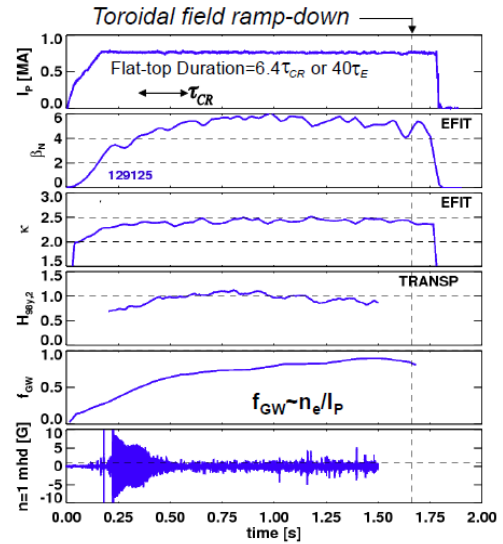


Figure 8 - From top to bottom, the plasma current (I_p), normalized β (β_N), boundary elongation (κ), confinement multiplier with respect to ITER-98y,2 scaling, Greenwald fraction (f_{GW}), and $n=1$ rotating MHD signature.

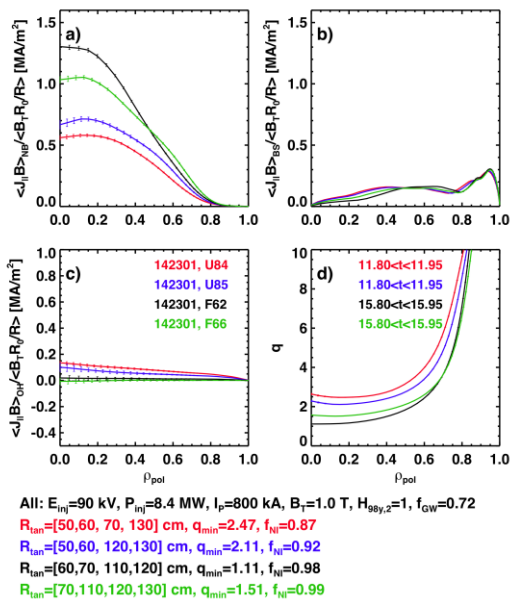
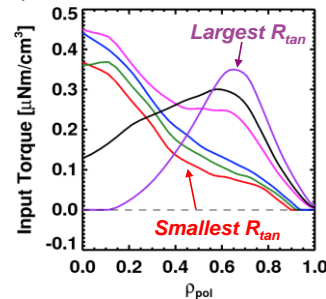


Figure 9 - Example of q_{\min} control using various combinations of 4 neutral beams. Shown are profiles of a) the NBCD, b) then bootstrap current, c) the ohmic current, and d) the safety factor. Note that the non-inductive fraction is greater than or equal to 87% for scenarios in this scan.

Torque Profiles From 6 Different NB Sources



Measured and Calculated NTV Torque Profiles

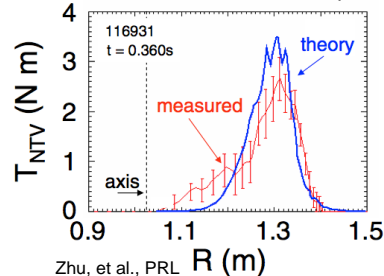


Figure 10 - The torque profiles for the six NSTX-U beam sources are shown at top, and the measured and modeled torque profiles for $n=3$ NTV braking are shown at bottom.

Many of the proposed scenarios for FNSF are at values of β_N beyond those which are stable for an equilibrium without nearby conductors. As a consequence, the resistive wall mode (RWM) will be a significant risk. Beyond the active stabilization noted in Section 3.9.2, an optimal rotation profile will significantly improve passive stability in this regime. As shown in Figure 10, NSTX-U will have important capabilities for modifying and controlling the rotation profile. The upper frame shows that the torque profiles for the six sources are quite different, with the small R_{tan} sources depositing torque on the magnetic axis and the large R_{tan} sources depositing torque at the mid-radius and beyond. The lower frame shows a measured and modeled neoclassical toroidal viscosity (NTV) torque profile, and represents the drag exerted on the plasma when 3D fields are applied. By varying the details of the applied field (toroidal mode number, for instance), it is possible to change the radial location of the peak drag torque.

If the proposed NCC coils are installed as anticipated, then even more flexibility in the torque profile may be expected. Together, the radially resolvable input and drag torque profiles will allow detailed experiments on the optimal rotation profile for sustained high- β_N steady state, from the perspective of both RWM elimination and transport optimization. Finally, the physics of rotation controllers will be synthesized and tested.

4.2. Develop first-wall and divertor solutions compatible with integrated high core performance

4.2.1. Develop high flux expansion integrated with partial detachment

Whereas the radiative divertor technique can be used for efficient divertor heat flux mitigation in combination with particle control, it is limited by the achievable divertor radiated power (atomic physics) and does not scale favorably to future MFE devices; thus, novel integrated approaches are sought. Several innovative divertor geometries with attractive heat flux handling properties have been proposed recently. One of them is a ‘snowflake’ divertor (SFD) configuration⁹⁶, which uses a second-order poloidal field null created by merging, or bringing close to each other, two first-order poloidal field null points (X-points) of a standard two-coil divertor configuration. In the snowflake divertor, the magnetic geometry is modified in several favorable ways that hold promise for steady-state divertor heat flux reduction, ELM peak heat flux reduction, and impurity erosion control. Experimental studies performed on NSTX indicated that the snowflake divertor may be a viable solution for the outstanding tokamak plasma-material interface issues^{96,97,98,99}. Experiments conducted in 4-6 MW NBI-heated H-mode plasmas demonstrated that the snowflake divertor configuration was compatible with high-confinement core plasma operation, while being very effective in steady-state divertor heat flux mitigation and impurity reduction. Peak divertor heat flux was reduced from 3-7 MW/m² to 0.5-1 MW/m². Additional seeding of deuterated methane increased divertor radiation further, demonstrating the potential for increased divertor radiative loss even

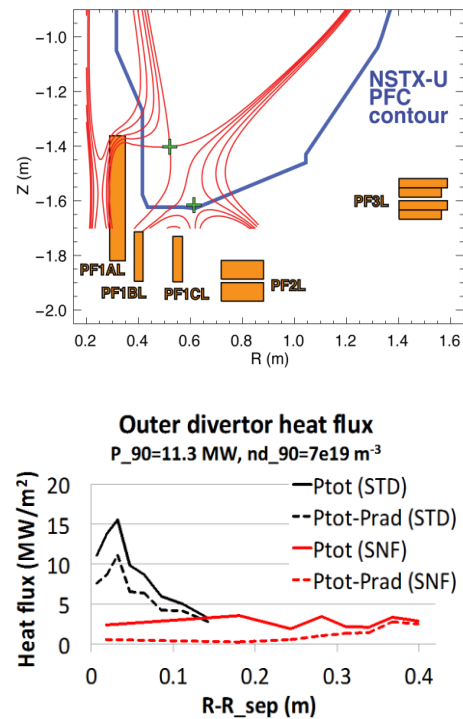


Figure 11 - Snowflake divertor geometry in NSTX-U (top panel), divertor heat flux profiles in standard (STD) and snowflake (SNF) divertors (bottom panel)

at higher scrape-off layer powers. Heat fluxes from Type I ELMs were also significantly dissipated: peak target temperatures measured at peak ELM times reached 1000-1200 degrees centigrade in the standard divertor phase and only 300-500 degrees centigrade in the SFD phase. H-mode core confinement was maintained during radiative detachment, and core carbon concentration was reduced by up to 50%.

Experimental results from NSTX favorably project the snowflake divertor properties to future high-power density devices, e.g., NSTX-U and ST-based FNSF. To enable these projections, a two-dimensional multi-fluid edge transport model based on the UEDGE code was developed and applied to modeled NSTX-U snowflake equilibria, yielding optimistic projections for the mitigated peak divertor heat flux (Fig. 11). In the NSTX-U, two up-down symmetric sets of four divertor coils will be used to test snowflake divertors for handling the projected steady-state peak divertor heat fluxes of 20-30 MW/m² in 2 MA discharges up to 5 s long with up to 12 MW NBI heating.

4.2.2. Explore high-Z PFCs for retention physics, sputtering, erosion, re-deposition and core impurity radiation, and the effects of high PFC operating temperature

Plasma wall interactions have a profound effect on the performance of present fusion machines and pose the critical challenge for next-step devices including ITER. To date NSTX has been lined with mostly ATJ graphite tiles however carbon influx has been an issue in ELM free plasmas¹⁰⁰. NSTX has also implemented a liquid lithium divertor (LLD) module to investigate the effects of liquid lithium in diverted H-mode plasmas¹⁰¹. In the next 5 year plan (2014-18), NSTX-U plans to implement a staged transition from graphite to molybdenum tiles on the upper and lower divertors and wall that will be coated with boron or lithium. We will investigate the effect of these low and high Z plasma facing materials on deuterium uptake, material migration, impurity influx and plasma performance under high heat flux conditions that are highly relevant to next step devices such as FNSF¹⁰². In the following 5 year plan (after 2018), NSTX-U intends to implement full high-Z PFC coverage – most likely by coating the remaining graphite tiles with tungsten or molybdenum.

4.2.3. Develop liquid lithium and other metals for surface replenishment to mitigate erosion and re-deposition and potential for resilience to off-normal events, and to control confinement

Significant uncertainty exists concerning the extrapolation of solid-PFCs to reactor-class devices. At present, advanced cooling schemes are operated at extremes to maintain surface temperatures to an acceptable level. In the face of transient power loading, such as during ELMs, local melting or other damage mechanisms may occur as a result. Cumulative wall erosion is expected to lead to 1000s of kgs of eroded material per operational year – a regime in which modern machines offer no practical experience. While there may be routes to disruption and other transient mitigation techniques, other problems, such as the net reshaping of PFCs, appear less tractable. A potentially game-changing technology is available in the form of liquid metal PFCs. These items eliminate net reshaping effects by allowing one to simply replace lost material or remove the excess by flow. Thermal stresses are eliminated in the liquid metal itself, which is the plasma-facing material. Liquid metals also separate the problem of neutron loading: the liquid itself is not subject to any net damage mechanism, though the substrate does suffer neutron damage. This allows one to study the PMI and neutron-effects separately. The NSTX program has pioneered the use of liquid-metal PFCs in a diverted, H-mode plasma through the use of the liquid lithium divertor. The NSTX-U plan is targeting the installation of a fully flowing, actively cooled liquid metal PFC module and further research on advanced PFC options for reactor-class devices (e.g. capable of operating with 10MW/m² peak divertor heat fluxes). NSTX-U provides an ideal test-bed with a large heating power concentrated in a relatively small major radius machine. In addition

to a reactor-relevant divertor power load, NSTX-U also has a high P/S ratio (roughly half that in an FNSF-type device) allowing full-machine erosion studies to be made alongside the relevant PFC technological advances.

We also note that all tokamaks, past and present – in fact, all magnetic confinement devices of any configuration – have operated in a small corner of edge plasma parameter space, as defined by $n_e(a)$ – the edge plasma density, $T_{e,i}(a)$ – the edge electron and ion temperature, and $n_o(a)$ – the edge neutral density, which is almost completely determined by recycling at the PFCs. This despite our understanding that core plasma performance, the free energy available to drive the microinstabilities that determine tokamak transport, and many of the MHD instabilities which limit tokamak operation are strongly dependent on edge plasma conditions. It has been shown¹⁰³ that the controlling parameter in the plasma edge is recycling; in a very low recycling plasma with core fueling, the edge density is predicted to drop, and the particle temperature should be comparable to the core. In principle, liquid lithium can produce a boundary which provides a recycling coefficient of as low as 10 – 20%. Therefore, in addition to performance enhancement, the use of liquid lithium PFCs can provide a strong test of our understanding of the plasma edge, and greatly extend the edge plasma operating space for tokamaks. In the small ST CDX-U, the use of liquid lithium PFCs has produced evidence of significant confinement enhancement in Ohmic discharges¹⁰⁴. This novel edge physics regime would provide a much broader test of edge models than is presently available, as well as an indication of whether core confinement will continue to improve as recycling is reduced to very low levels.

An alternative liquid metal which does not retain hydrogen, and is expected to provide recycling characteristics similar to high-Z solids, is tin. Although tin is not expected to enhance discharge performance, the absence of tritium retention in liquid tin, as opposed to liquid lithium, would greatly reduce concerns over tritium inventory, both in the liquid metal PFC and in the remainder of the tokamak structure. Tin also has far lower vapor pressure than lithium, with an upper operating temperature limit in the range of 900 C. However, liquid tin has never been employed as a PFC in any tokamak. LTX has limiter systems capable of operating with liquid tin for a first test. *For additional information on liquid metal research, see the whitepaper submitted by M. Jaworski et al.*

5. Utilization of the ST to advance fusion materials science and harness fusion power

5.1. The ST as a compact fusion neutron source, fusion nuclear science facility, and pilot plant

The ST has long been recognized to have the potential to provide a compact fusion neutron source for a range of fusion applications. The low aspect ratio of the ST provides a reduced surface area to volume ratio, and also enhanced neutron flux peaking on the outboard side. As a result, the ST



Figure 12 – Example ST devices ranging from smaller to larger in size and with increasing fusion power and performance.

configuration can provide high neutron wall loading $> 1\text{MW/m}^2$ needed for fusion nuclear component testing¹⁰⁵ with modest device sizes with plasma major radius in the range of 1 to 2m. A potential advantage of the small ST is reduced fusion power and tritium consumption for a given neutron wall loading that could reduce/remove the requirement for tritium self-sufficiency during the component

development and testing phase. Additional information on ST applications and research needs can be found in the FESAC toroidal alternates panel report (2008) and the ReNeW report (2009).

Proposed ST applications and configurations (see Figure 12) range from a neutron source and fusion-fission demonstration experiments¹⁰⁶ (Russia), a component test facility¹⁰⁷ (Culham, UK), compact fusion neutron source and fusion-fission hybrid¹⁰⁸ (UT-Austin), fusion nuclear science facility¹⁰⁹ and component test facility¹¹⁰ (ORNL), and an ST pilot plant with FNSF/CTF capabilities which also ultimately targets net electricity production¹¹¹ (PPPL). All tokamak/ST based steady-state neutron sources share the need for non-inductive plasma current sustainment as described in previous sections. However, the ST is unique in that it would operate without inductive current drive from an ohmic heating solenoid, and thus non-inductive plasma start-up and ramp-up are also required as described below.

5.2. The unique challenge of an ST-based FNSF: non-inductive plasma start-up and ramp-up

The low aspect ratio of the ST leaves little room for an Ohmic transformer or nuclear shielding for the central column. Some of the required volt-seconds required for plasma formation could potentially be applied using an iron core transformer or a mineral-insulated solenoid, but these concepts require further evaluation, design, and development. Alternative non-solenoidal approaches for plasma start-up include coaxial helicity injection (CHI), plasma gun start-up, and the use of the outer poloidal field coil set to generate a toroidal electric field or current overdrive using bootstrap current and/or RF current drive. Beyond plasma start-up, an ST-FNSF also requires non-inductive ramp-up to the full operating current. A critical issue will be the gap in plasma current (fast-particle confinement) and density (ionization distance) where neutral beam injection (NBI) can be effectively employed. Sufficient thermal confinement is also required to provide a target consistent with high efficiency current drive and high bootstrap fraction.

5.2.1. Coaxial Helicity Injection (CHI)

Plasma start-up using Coaxial Helicity Injection (CHI - see Figure 13) is one method for eliminating the solenoid. Considerable progress has been made in this area to suggest that this is a viable method for solenoid-less plasma startup in a tokamak^{112,113}. Transient CHI was first developed on the HIT-II ST at the University of Washington and then tested and further improved on the much larger NSTX device at PPPL. These results coupled with recent simulations with the TSC code have revealed many important aspects of CHI physics and its application to future machines. The key results are briefly summarized below.

NSTX and HIT-II, two machines of vastly different size (NSTX plasma volume is 30 times that of HIT-II), have both achieved significant levels of start-up current through CHI. 300 kA start-up current has been

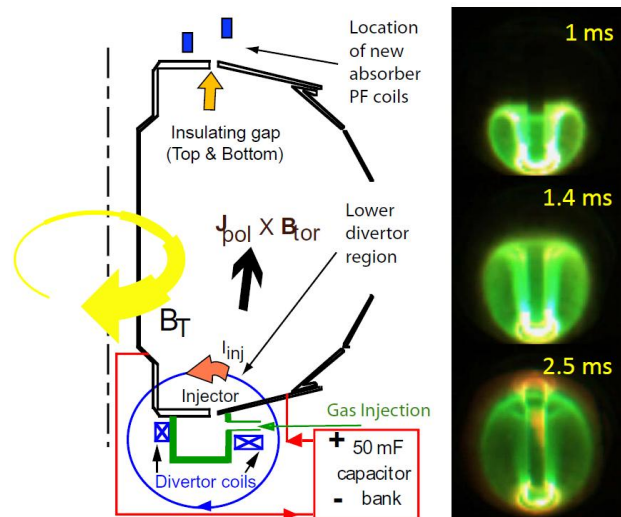


Figure 13 – (left) schematic and (right) camera images of Coaxial Helicity Injection (CHI) plasma start-up in NSTX.

demonstrated on NSTX. On NSTX, the method is highly efficient, producing more than 10 Amps/Joule of initial stored capacitor bank energy. The scaling to larger machines with higher toroidal field is quite favorable: NSTX achieves 10 times the current multiplication factor of HIT-II. Current multiplication is defined as the ratio of the CHI produced plasma current to injected current, which is about 70 in NSTX. In addition, the CHI generated plasmas on NSTX have desirable properties including low normalized internal inductance of 0.35, low electron density and low impurity content, as needed for subsequent non-inductive current ramp-up using NBI and RF waves. Simulations with the TSC code show agreement with the theoretical prediction for CHI as it is scaled to larger machines.

The conditions and capabilities of CHI on NSTX-U will be enhanced to include the following capabilities. First, NSTX-U is planning to have a 1 MW ECH capability that would increase the electron temperature of the CHI target as needed for direct coupling to neutral beams. Second, the factor of two increase in the toroidal field from the center-stack upgrade will further increase the current multiplication factor and allow more poloidal flux to be injected at a given injector current. Further, the injected poloidal flux capability in NSTX-U is more than 2.5 times that in NSTX, which will allow NSTX-U to generate well in excess of 400kA start-up current, enough so that neutral beams can efficiently couple to the plasma discharges. Lastly, NSTX-U will incorporate metallic divertor plates, which should further improve plasma start-up by CHI by reducing low-Z impurities.

The enhancement of CHI capability on NSTX-U should allow for a demonstration of full non-inductive start-up and non-inductive current ramp-up. NSTX-U is thus uniquely positioned in the world to demonstrate this long-sought capability for tokamak/ST-based systems. Such a demonstration would pave the way for future tokamak/ST based systems to be built at lower cost, and with increased optimization of the aspect ratio, which should result in a more efficient FNSF and/or fusion power plant. *Additional information on CHI is provided in a whitepaper submitted by R. Raman.*

5.2.2. Point helicity injection (“plasma guns”)

In this method of plasma current formation, current is injected into a pre-programmed vacuum helical magnetic field. With high injection current and modest B-field strength, the filaments merge into a current sheet, and with lower B-field, the current-driven poloidal field overwhelms the vacuum vertical field leading to relaxation via MHD activity to a tokamak-like Taylor state with high toroidal current multiplication (see Figure 14). This technique has generated solenoid-free plasma start-up current exceeding 100kA on the Pegasus Toroidal Experiment. The maximum plasma current achievable with the injection technique has been shown to scale as $(I_{TF} I_{INJ})^{1/2}$ consistent with helicity balance relations and Taylor relaxation criteria. Thus, the current formation capability of this technique is also expected to scale favorably with the increased toroidal field of larger next-step ST devices. This technique may be particularly attractive for nuclear devices such as FNSF, since the plasma gun sources can be retracted or removed after the plasma start-up phase. Tests of plasma gun start-up in the larger NSTX-U device are planned during the next 5 year period of operation.

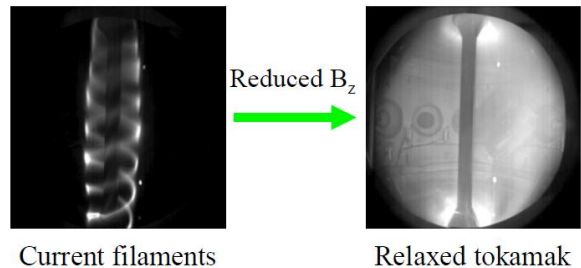


Figure 14 – Example of point helicity injection plasma current start-up on the Pegasus Toroidal Experiment.

5.2.3. HHFW for current ramp up

High-harmonic fast wave (HHFW) power can, in principle, effectively ramp-up the plasma current in an FNSF device, even at low plasma currents where neutral beam current drive is ineffective due to poor fast-ion confinement. HHFW power is also a good candidate for core non-inductive current generation in future fusion reactors. HHFW experiments in NSTX have demonstrated that only 1.4 MW of HHFW power can generate and sustain an H-mode plasma with a plasma current of 300 kA and a non-inductive plasma current fraction of 0.7 – 1, where about 30% of the plasma current is driven directly by fast waves and the rest is bootstrap current¹¹⁴. HHFW experiments planned for NSTX-U will use much higher RF power and are predicted to demonstrate fully non-inductive plasma current ramp up and significant on-axis HHFW current drive in the H-mode regime. The results from NSTX-U HHFW experiments will be compared to predictions from advanced RF numerical simulations. Following the validation of advanced RF models using NSTX-U HHFW experiments, these models will be used to predict the HHFW performance in an FNSF, ITER, and other future fusion reactors.

5.2.4. ECH/EBW for plasma initiation, current drive in over-dense conditions

An FNSF-ST device will operate in a plasma regime where the local electron plasma frequency far exceeds the electron cyclotron frequency. This “overdense” plasma regime precludes the use of conventional electron cyclotron heating (ECH) and electron cyclotron current drive (ECCD) to assist fully non-inductive plasma current ramp-up and to suppress deleterious off-axis neoclassical tearing mode activity. In the overdense plasma regime electron Bernstein wave heating (EBWH) can provide efficient local electron heating and EBW current drive (EBWCD) with efficiencies that are better than the ECCD efficiencies achieved in “underdense” tokamak plasmas^{115,116}. To enable EBWH and EBWCD, the RF power is launched from external mirrors or waveguide arrays and is coupled to EBWs inside the overdense plasma via mode conversion, that typically occurs in the plasma scrape-off layer (SOL) near the last closed flux surface. Experiments on NSTX clearly demonstrated that the EBW mode conversion efficiency is significantly improved in the H-mode regime by using lithium wall conditioning to mitigate RF power losses in the SOL that occur as a result of collisions near the EBW mode conversion layer^{117,118}. A 2 MW, 28 GHz ECH/EBWH system is planned for installation on NSTX-U after it begins operation. This heating system will initially be used to study ECH-assisted non-inductive ST plasma initiation. Later a steerable mirror launcher will be installed for EBW heating and current drive during the plasma current flat top. These NSTX-U ECH/EBWH experiments will use lithium wall conditioning, and will provide an experimental validation of advanced RF codes that will in turn be used to predict ECH/EBWH performance in FNSF.

5.2.5. NBI-driven current ramp-up

The primary heating and current-drive system proposed for most ST-based FNSFs is neutral beam injection (NBI). For ST-FNSF, it is envisioned that a ~1MA target plasma will be ramped up to a flat-top current value of approximately 8-12MA (depending on the chosen FNSF operating point) using NBI heating and current drive in combination with H-mode operation and high bootstrap fraction. A key issue for such a scenario is determining beam and plasma parameters which provide a good match to both the initial and final plasma conditions. In particular, good fast ion confinement by the low current and low density target plasma is required to effectively absorb the NBI. On NSTX, the NBI injection was generally too perpendicular to provide good fast ion confinement at low current (< 0.6-0.7MA), and non-inductive ramp-up studies could not be performed. In NSTX-U, through the addition of a more tangential

NBI, fast-ion confinement is projected to be substantially improved at low current and density, and good (>80%) fast-ion absorption is projected for currents as low as 0.4MA. TRANSP and TSC simulations indicate that with this capability, studies of plasma current ramp-up from 0.4 to 1MA should be possible. Such studies will serve as a strong test of the viability of NBI to ramp-up the plasma current to high values as needed for an ST-based FNSF. For more details, see Reference 1.

5.3. Role of NSTX-U in support of prototyping ST-FNSF operational scenarios

Based upon all the above contributions and capabilities, NSTX-U will contribute to key physics studies for many issues of relevance to the FNSF fusion core. With regard to the high- β plasmas, NSTX-U will establish a physics basis for scaling transport to higher field and current, error field correction and RWM control, and current drive physics for steady-state operation. Furthermore, NSTX-U will examine a range of solutions to well known divertor issues, including the development of high-performance scenarios with metallic PFCs and heat flux reduction through advanced divertor geometry (snowflake divertor) and controlled divertor radiation. Finally, NSTX-U will address critical issues of start-up and ramp-up for the ST-FNSF concept. This research strongly complements ITER and FNSF research at conventional aspect ratio, and provides critical support for evaluating the low-aspect ratio concept for an FNSF.

References

- ¹ J. E. Menard, et al., Nucl. Fusion **52** 083015 (2012)
- ² F. Najmabadi, et al., Fusion Engineering and Design **65** (2003) 143-164
- ³ J. E. Menard, et al., Nucl. Fusion **51** (2011) 103014
- ⁴ S. Nishio, et al., IAEA-FEC 2003, http://www-pub.iaea.org/mtcd/publications/pdf/csp_019c/pdf/ftp1_21.pdf
- ⁵ K. Tobita, et al., Journal of Nuclear Materials **329–333** (2004) 1610–1614
- ⁶ T. Nishitani, et al., Fusion Engineering and Design **81** (2006) 1245–1249
- ⁷ K. Tobita, et al., Nucl. Fusion **47** (2007) 892–899
- ⁸ A. Fasoli, et al., Nucl. Fusion **47** S264-S284 (2007)
- ⁹ N. N. Gorelenkov, et al., Nucl. Fusion **43** 594 (2003)
- ¹⁰ N. N. Gorelenkov, et al., Nucl. Fusion **45** 226 (2005)
- ¹¹ S. P. Gerhardt, et al., Nucl. Fusion **51** 033004 (2011)
- ¹² J. W. Berkery, et al., Phys. Plasmas **17** 082504 (2011)
- ¹³ N. A. Crocker, et al., Phys. Rev. Lett. **97** 045002 (2006)
- ¹⁴ M. Podestà, et al., Phys. Plasmas **17** 122501 (2010)
- ¹⁵ M. Podestà, et al., Nucl. Fusion **51** 063035 (2011)
- ¹⁶ N. N. Gorelenkov, et al., Phys. of Plasmas **16** 056107 (2009)
- ¹⁷ D. Stutman, et al., Phys. Rev. Lett. **102** 115002 (2009)
- ¹⁸ E. D. Fredrickson, et al., Phys. Plasmas **16** 122505 (2009)
- ¹⁹ E. D. Fredrickson, et al., Nucl. Fusion **52** 043001 (2012)
- ²⁰ S. S. Medley, et al., Nucl. Fusion **52** 013014 (2012)
- ²¹ E. D. Fredrickson, et al., Nucl. Fusion **52** 043001 (2012)
- ²² M. Podestà, et al., Nucl. Fusion (in press, 2012)
- ²³ E. D. Fredrickson, et al., Phys. Plasmas **13** 056109 (2006)
- ²⁴ M. Podestà, et al., Phys. Plasmas **16** 056104 (2009)
- ²⁵ D. S. Darrow, et al., Nucl. Fusion (submitted, 2012)
- ²⁶ J. E. Menard, et al., Nucl. Fusion **52** 083015 (2012)
- ²⁷ N. A. Crocker, et al., Plasma Phys. Control. Fusion **53** 105001 (2011)
- ²⁸ D. R. Smith, et al., Rev. Sci. Instrum. **83** 10D502 (2012)

- ²⁹ M. Podestà, et al., Rev. Sci. Instrum. **79** 10E521 (2008)
- ³⁰ A. Bortolon, et al., Rev. Sci. Instrum. **81** 10D728 (2010)
- ³¹ D. Liu, et al., Rev. Sci. Instrum. **77** 10F113 (2006)
- ³² S. S. Medley, et al., Rev. Sci. Instrum. **75** 3625 (2004)
- ³³ W. U. Boeglin, et al., Rev. Sci. Instrum. **81** 10D301 (2010)
- ³⁴ N. J. Fisch Nucl. Fusion **40** (2000) 1095 (2000)
- ³⁵ H. Doerk et al., Phys. Rev. Lett. **102** 155003 (2011)
- ³⁶ K.L. Wong et al., PPPL report PPPL-4579 (2011)
- ³⁷ W. Guttenfelder et al., Phys. Plasmas **19** 022506 (2012)
- ³⁸ K.L. Wong et al., Phys. Rev. Lett. **99**,35003 (2007); Phys. Plasmas **15** 056108 (2008)
- ³⁹ W. Guttenfelder et al., Phys. Rev. Lett. **106** 155004 (2011); Phys. Plasmas **19** 056119 (2012)
- ⁴⁰ S.M. Kaye et al., Nucl. Fusion **47** 499 (2007)
- ⁴¹ J. Zhang et al., Rev. Sci. Instrum **81** 10D519 (2010)
- ⁴² E. Mazzucato et al., Phys. Rev. Lett. **101**, 075001 (2008)
- ⁴³ D.R. Smith, et al., Phys. Rev Lett. **102**, 225005 (2009)
- ⁴⁴ Y. Ren, et al, Phys. Rev. Lett. **106**, 165005 (2011)
- ⁴⁵ Y. Ren, et al, Phys. Plasmas **19** 056125 (2012)
- ⁴⁶ D. Stutman, et al., Phys. Rev. Lett. **102**, 115002 (2009)
- ⁴⁷ N. Gorelenkov, et al., Nucl. Fusion **50** (2010) 084012
- ⁴⁸ J.C. Hosea et al., AIP Conf Proceedings 105 1187 (2009)
- ⁴⁹ G. Taylor et al., Physics of Plasmas **17** 056114 (2010)
- ⁵⁰ R.J. Perkins et al., Phys. Rev. Lett. **109** 045001 (2012)
- ⁵¹ D.L. Green et al., Phys. Rev. Lett. **107** 145001 (2011)
- ⁵² R. Maingi, et al., Nucl. Fusion **50** 064010 (2010)
- ⁵³ S.M. Kaye S.M., et al Nucl. Fusion **51**, 113019 (2011)
- ⁵⁴ J.E. Kinsey et al.,Nucl. Fusion **51**, 083001 (2011)
- ⁵⁵ T.E. Evans et. al., Nature Phys **2** 419 (2006)
- ⁵⁶ W. Suttrop et al., Plasma Physics Control. Fusion **53** 124014 (2011)
- ⁵⁷ J.M. Canik, et al., Phys. Rev. Lett. **104** 045001 (2010)
- ⁵⁸ J.M. Canik, et al., Nucl. Fusion **50** 0641016 (2010)
- ⁵⁹ J.M. Canik, et al., Nucl. Fusion **52** 054001 (2012)
- ⁶⁰ J.-K. Park, et al., Phys. Rev. Lett. **102** 065002 (2009)
- ⁶¹ D.K. Mansfield, et al., J. Nucl. Mat. **390-391** 764 (2009)
- ⁶² R. Maingi, et al., Phys. Rev. Lett. **103** 075001 (2009)
- ⁶³ J.M. Canik, et al., Phys. Plasmas **18** 056118 (2011)
- ⁶⁴ R. Maingi, et al., Phys. Rev. Lett. **107** 145001 (2011)
- ⁶⁵ L.R. Baylor, et al., Phys. Plasmas **7** 1878 (2000)
- ⁶⁶ V. A. Soukhanovskii, et al., Phys. Plasmas **16** 022501 (2009)
- ⁶⁷ V. A. Soukhanovskii, et al., Nucl. Fusion **49** 095025 (2009)
- ⁶⁸ V. A. Soukhanovskii, et al., 39th EPS Conference, Stockholm, Sweden, 2-6 July 2012, Paper P-5.049
- ⁶⁹ V. A. Soukhanovskii et al., Review of Scientific Instruments **83** 10D716 (2012)
- ⁷⁰ J-W. Ahn, et al., Nucl. Fusion **50** 045010 (2010)
- ⁷¹ J-W. Ahn, et al., Phys. Plasmas **18** 056108 (2011)
- ⁷² J-W. Ahn, et al., Rev. Sci. Instrum. **81** 023501 (2010)
- ⁷³ K.F. Gan, et al., submitted to Rev. Sci. Instrum. (2012)
- ⁷⁴ J.-K. Park, et al., Phys. Rev. Lett. **9** 195003 (2007)
- ⁷⁵ J.-K. Park, et al., Phys. Plasmas **1**, 082512 (2009)
- ⁷⁶ J.-K. Park, et al., Phys. Plasmas **1**, 052110 (2007)
- ⁷⁷ J. E. Menard (PI), et al., ITER IPEC Task Agreement on Error Field Correction (2010)
- ⁷⁸ J.-K. Park, et al., Phys. Rev. Lett. **10**, 065002 (2009)

- ⁷⁹ W. M. Solomon et al., Phys. Rev. Lett. **101** 065004 (2008)
- ⁸⁰ S. M. Kaye et al., Nucl. Fusion **49** 045010 (2009)
- ⁸¹ J.-K. Park et al., Submitted to Nucl. Fusion (2012)
- ⁸² J.E. Menard, et al., Phys. Rev. Lett. **97** 095002 (2006).
- ⁸³ S.P. Gerhardt, et al., Nucl. Fusion **51** 033004 (2011)
- ⁸⁴ S.P. Gerhardt, et al., Nucl. Fusion **51** 073031 (2011)
- ⁸⁵ S.A. Sabbagh, et al., Phys. Plasmas **9** 2085 (2002)
- ⁸⁶ S.A. Sabbagh, et al., Nucl. Fusion **46** 635 (2006)
- ⁸⁷ A.C. Sontag, et al., Phys. Plasmas **12** 056112 (2005)
- ⁸⁸ S.A. Sabbagh, et al., Nucl. Fusion **50** 025020 (2010)
- ⁸⁹ J.W. Berkery, et al., Phys. Rev. Lett. **104** 035003 (2010)
- ⁹⁰ J.W. Berkery, et al., Phys. Plasmas **17** 082504 (2010)
- ⁹¹ S.A. Sabbagh, et al., Phys. Rev. Lett. **97** 045004 (2006)
- ⁹² O.N. Katsuro-Hopkins, et al., Nucl. Fusion **47** 1157 (2007)
- ⁹³ O.N. Katsuro-Hopkins, S.A. Sabbagh, J.M. Bialek, "Analysis of resistive wall mode LQG control in NSTX with mode rotation", Proc. of 48th IEEE Conference on Decision and Control, Shanghai, China, 2009, paper WeA09.5.
- ⁹⁴ J.E. Menard, et al., Nucl. Fusion **50** 045008 (2010)
- ⁹⁵ J.E. Menard, et al., Nucl. Fusion **52** 083015 (2012)
- ⁹⁶ D. Ryutov, Phys. Plasmas **14** 064502 (2007)
- ⁹⁷ V. Soukhanovskii, et al., J. Nucl. Mater. **415** S365 (2011)
- ⁹⁸ V. Soukhanovskii, et al., Nucl. Fusion **51** 012001 (2011)
- ⁹⁹ V. A. Soukhanovskii, et al., Phys. Plasmas **19** 000000 (2012)
- ¹⁰⁰ R. Raman, Nucl. Fus. **51** 094011 (2011)
- ¹⁰¹ H.W. Kugel et al., Fus. Eng. & Des. in press (2011)
- ¹⁰² J.E. Menard et al., Nucl. Fus. **51** 103014 (2011)
- ¹⁰³ . I. Krasheninnikov et al., Phys. Plasmas **10** 1670 (2003)
- ¹⁰⁴ R. Majeski et al., Phys. Rev. Lett. **97** 075002 (2006)
- ¹⁰⁵ M. Abdou et al., Fusion Technology **29**, 1 (1996)
- ¹⁰⁶ B. Kuteev, et al, Nucl. Fusion **51** 073013 (2011)
- ¹⁰⁷ G. M. Voss, et al, Fusion Engineering and Design **83** 1648–1653 (2008)
- ¹⁰⁸ M. Kotschenreuther, et al., Fusion Engineering and Design **84** 83–88 (2009)
- ¹⁰⁹ Y-K M. Peng, et al., Fusion Science and Technology **56**, 957 (2009)
- ¹¹⁰ Y-K M. Peng, Plasma Phys. Control. Fusion, **47** B263–B283 (2005)
- ¹¹¹ J.E. Menard et al., Nucl. Fus. **51** 103014 (2011)
- ¹¹² R. Raman, et al, Phys. Rev. Lett. **90**, 075005 (2003)
- ¹¹³ R. Raman, et al., Phys. Rev. Lett. **104** 095003 (2010)
- ¹¹⁴ G. Taylor, et al., Phys. Plasmas **19** 042501 (2012)
- ¹¹⁵ G. Taylor, et al., Phys. Plasmas **11** 4733 (2004)
- ¹¹⁶ J. Urban, et. al., Nucl. Fusion **51** 083050 (2011)
- ¹¹⁷ S. J. Diem et al., Phys. Rev. Lett. **103** 015002 (2009).
- ¹¹⁸ S. J. Diem et al., Nucl. Fusion **49** 095027 (2009)